Coupled QM/MM Molecular Dynamics Simulations of HCl Interacting with Ice Surfaces and Water Clusters − Evidence of Rapid Ionization

Marcus Svanberg,[†] Jan B. C. Pettersson,*[,†,§] and Kim Bolton[†,‡]

Department of Chemistry, Physical Chemistry, Göteborg University, SE-412 96 Göteborg, Sweden, School of Engineering, University of Borås, SE-501 90 Borås, Sweden, and School of Environmental Sciences, Göteborg University, SE-412 96 Göteborg, Sweden.

Received: March 28, 2000

We present the results of coupled quantum mechanics and molecular mechanics (QM/MM) classical molecular dynamics simulations for HCl sticking to the (0001) basal plane of ice Ih. Interatomic forces and energies of hydrogen chloride and up to 24 water molecules in the top ice bilayer were obtained from semiempirical molecular orbital calculations based on the PM3 method. A few PM3 parameters were adjusted so that structural and energetic properties of small neutral and ionic systems match available ab initio and experimental data. This QM region was coupled to the remainder of the ice surface (the MM region), which was treated using the analytic TIP4P force field. The surface temperature was between 0 and 180 K, and the dynamics was followed for 100 ps. On surface impact, HCl binds to a dangling (free) H_2O oxygen via a $ClH-OH_2$ hydrogen bond. If the Cl is solvated by one dangling H_2O hydrogen, HCl adsorbs molecularly. If two dangling hydrogens are available in a surface hexagon, HCl dissociates to a $Cl^- - H_3O^+$ contact ion pair. The simulations thus predict a mechanism by which HCl can ionize readily on ice surfaces. This mechanism is consistent with a saturation coverage of 0.33 monolayers for ionized HCl on ice surfaces. As a comparison we have also simulated HCl colliding with a cubic $(H_2O)_8$ cluster, in which the whole system was treated by the semiempirical method. Hydrogen chloride adsorbs on the cluster and, depending on the temperature, the $(H_2O)_8$ cube may open up, thereby initiating HCl ionization. The results are discussed in relation with stratospheric heterogeneous ozone chemistry and available experimental and theoretical results.

1. Introduction

Since the discovery of the ozone hole over Antarctica,[1] heterogeneous processes have been recognized as playing a key role in the chemistry of the stratosphere. The annual rapid depletion of ozone occurs in the presence of polar stratospheric cloud (PSC) particles, which provide surfaces for catalyzing important chemical reactions. The composition and structure of PSC particles, which are determined by equilibrium parameters such as local temperature and partial pressure of condensable molecules, as well as kinetically driven processes,[2a−b] have been the focus of recent discussion.[2a] Recent field measurements performed at an altitude of 20−24 km showed that, between 188 and 195 K, PSCs consist primarily of H_2O and HNO_3, with an H_2O:HNO_3 molar ratio greater than ten.[2c] These PSCs are thus not nitric acid tri-, di- or monohydrate particles. The observations suggest that, in this temperature range, the PSCs are an $H_2O-HNO_3-H_2SO_4$ ternary solution.[2a,c] Although this study showed that decreasing temperature leads to increasing H_2O:HNO_3 molar ratio, no measurements were made below the ice frost point. At these lower temperatures, PSCs may be composed mainly of water ice (type II) or solid particles consisting of H_2O condensed on binary/ternary nucleation sites.[2a]

The rate of the reaction

$$ClONO_2 + HCl \rightarrow Cl_2 + HNO_3 \qquad (1)$$

is greatly enhanced in the presence of PSC particles.[3] Both HCl and $ClONO_2$ are important chlorine "reservoir" compounds and react to form molecular chlorine which photodissociates, thereby initiating catalytic gas-phase ozone destruction cycles.[3] On water-rich surfaces chlorine nitrate hydrolyzes to HOCl, which can subsequently react with HCl, but under strongly acidic conditions $ClONO_2$ can react directly with HCl.[3−6] Recent ab initio studies which show that $ClONO_2$ ionizes spontaneously when embedded in an ice cluster are consistent with these observations.[7] Hydrogen chloride is believed to be ionically dissolved in PSC particles by the step

$$HCl + H_2O \rightarrow Cl^- + H_3O^+ \qquad (2)$$

i.e., analogous to the situation in water solutions of hydrochloric acid. Experiments have shown that gaseous HCl efficiently sticks to ice surfaces in quantities equivalent to the order of one monolayer,[6,8,9] and infrared spectroscopy studies indicate the presence of hydronium ions at the surface.[5,10] However, the molecular mechanism of reaction 2 has been under considerable debate. Molecular dynamics (MD) simulations of Clary, Kroes, and co-workers[11−14] have shown that the trapping coefficient, i.e., the probability that HCl does not scatter directly off the surface, is high. This is in agreement with molecular beam experiments[15−17] which predict a sticking (or uptake) coefficient close to one for HCl on pure ice surfaces. However, the residence time for trapped molecular HCl on an ice surface has been estimated to be relatively short at 190 K.[13] Optical interference measurements by George and co-workers[18] have shown that ice surfaces are very dynamic under stratospheric conditions, with H_2O residence times on the surface as short as

* Telephone: +46-31-7722828. Fax: +46-31-7723107. E-mail: janp@phc.chalmers.se

[†] Department of Chemistry, Physical Chemistry, Göteborg University.

[§] School of Environmental Sciences, Göteborg University.

[‡] University of Borås.

10.1021/jp0012698 CCC: $19.00
Published on Web 06/15/2000

10^{-3} to 10^{-1} s. This observation was exploited by Hynes and co-workers,[19,21] who assumed that HCl remains adsorbed on the ice surface sufficiently long to be incorporated in the ice lattice by condensing H_2O molecules. They have shown that if an HCl molecule is inserted in the top bilayer of the ice lattice, replacing an H_2O molecule, then reaction 2 is thermodynamically favorable and proceeds rapidly. Although the mechanism proposed by Hynes and co-workers may be important under stratospheric conditions, condensation of gaseous water is not necessary for HCl ionization, which is also observed on low-temperature ice surfaces under vacuum.[10,22]

We have previously used classical MD simulations to study the dynamics of argon scattering from ice surfaces.[23,24] These simulations, as well as the present ones, were carried out concurrently with molecular beam experiments on the Ar−ice[25a] and HCl−ice[17] systems. The present theoretical work is concerned with the interaction between HCl and the basal surface of hexagonal ice, used as a model of a PSC type II particle. Although the precise (surface) structures of PSC particles are not known,[2b] and cubic and various amorphous forms of ice can be prepared at low temperature,[25b] hexagonal ice is the thermodynamically stable form below the ice frost point. The adopted model is therefore an appropriate starting point for theoretical investigation.[20] We focus on possible mechanisms for reaction 2 and subsequent dynamics of the product ions. By increasing the temperature, which leads to some reconstruction of the ideal hexagonal surface, and by comparing with HCl ionization in a cubic $(H_2O)_8$ cluster, we also show that the qualitative features of reaction 2 are insensitive to the precise structure of the ice.

The coupled QM/MM technique[26] is used for the present simulations. In this technique the chemical system is divided into two regions. Simulation of (groups of) atoms in the MM region is based on an analytic potential energy surface (PES), and atoms in the QM region are propagated using forces obtained directly from electronic structure calculations performed at each trajectory step. Atomic motion in the reactive QM region is geometrically constrained by being mechanically embedded in the MM region.[27] The MM atoms may also polarize the QM atoms, which is referred to as electronic embedding.[27] Thus, one combines the advantages of multidimensional trajectory simulation (where no degrees of freedom need be constrained) with direct dynamics[28] treatment of the QM region. The direct dynamics method yields the exact classical dynamics for a chosen level of electronic structure theory and, in principle, does not require prior knowledge of the important reaction channels (which is required when fitting an analytic PES).

The QM/MM and direct dynamics techniques have previously been used to study H_2O and HCl/H_2O systems.[29−32] For example, Laasonen and Klein[30] studied the structure of hydrochloric acid solutions with Car−Parrinello direct dynamics based on density functional theory. Coupled QM/MM Monte Carlo simulations of $HCl(H_2O)_{n\leq 24}$ clusters by Estrin et al.,[32] where HCl and one water molecule constituted the QM region, showed that HCl ionization depends on its position in the cluster.

In the present simulations the primary $HCl(H_2O)_n$ reaction center, which includes up to 24 water molecules, is treated within a semiempirical molecular orbital formalism. The quality of the PES in the QM region was improved by tuning a few PM3 parameters so that energies and geometries of small cluster systems agreed with published ab initio and density functional theory values. The QM region is electronically embedded in a TIP4P[33] ice surface. This coupled QM/MM system was used to simulate the trapping, solvation, and ionization of HCl on an ice surface, over 100 ps time scales. We regard the model applied here as an important complement to previous theoretical approaches.[11,13,19−21,31,32,34,35]

The remainder of the article is organized as follows: In the next section the QM and QM/MM methods are described together with the MD procedure. The simulation results are presented in section 3, and in section 4 they are discussed in relation to available data from the literature and stratospheric heterogeneous processes. The main conclusions of this work are given in section 5.

2. Model and Calculations

The coupled QM/MM classical MD method was used to simulate HCl colliding with the (0001) basal plane of ice Ih. The HCl molecule and 12 or 24 H_2O molecules in the top ice bilayer formed the QM region and were embedded in a periodic TIP4P ice surface.[33] Direct dynamics simulations[28] were performed for HCl collisions with a cubic $(H_2O)_8$ cluster, in which the whole system was treated by the semiempirical method. This cluster was chosen because of the structural similarities with the top bilayer of an ideal ice Ih basal surface; each molecule in the cubic cluster has 3-fold coordination, and every second molecule has a dangling (non-hydrogen bonding) hydrogen while the rest have a dangling (free electron lone pair) oxygen. Optimizations and tests on clusters were carried out with the MOPAC program.[36] The MD simulations and all calculations involving a QM/MM coupling were performed with the MOPS suite of programs.[37]

2.1. QM Method. In the present study we use the semiempirical RHF PM3 method[38] to describe the interaction between HCl and ice surfaces or water clusters. Although density functional and ab initio methods may provide more accurate results for small systems, the computational expense is normally several orders of magnitude larger than for semiempirical methods, especially if large basis sets are required.[39,40] In addition, high-level ab initio methods scale very unfavorably with system size, making them unsuitable for simulations where the QM system is large. The PM3 method was preferred over the MNDO[41] and AM1[42] semiempirical methods,[43] since it describes hydrogen bonding well, in particular for water clusters.[44,46] We have also modified a few PM3 parameters so that geometries and energies of small $(H_2O)_n$, $H^+(H_2O)_n$, and $HCl(H_2O)_n$ clusters agree with ab initio data available in the literature. The optimization of PM3 parameters, which is described below, provides a new set of parameters that are specific for the HCl−ice system and will be referred to as PM3-SSP (system specific parameters).[47]

Semiempirical molecular orbital methods are based on a minimal basis set for the valence electrons within the Hartree−Fock formalism.[48] The general idea behind semiempirical methods has been to generate a set of universal parameters which reproduce experimental data of a wide range of molecules.[38] Properties of other molecules can then be predicted with some confidence. Due to the parametrization, which to a certain extent compensates for the neglect of correlation, small basis set, etc., semiempirical schemes have generally been successful, although a number of deficiencies are well known.[38] A few studies, however, have abandoned the idea of using universal parameters.[47,49,50] Bash et al.[47] recently reoptimized AM1 parameters for the reactants and products in the proton transfer between methanol and imidazole and obtained an accurate free energy change for this process in aqueous solution. Rossi and Truhlar[49] modified the AM1 parameters using a small number points along

TABLE 1: Equilibrium Properties of Small H_2O Systems (bond lengths (r) in Ångström, angles (θ) in degrees, dissociation energies (E_d) in kJ/mol)

	H_2O		$(H_2O)_2$			H_3O^+			$H_5O_2^+$		
	r_{O-H}	θ_{HOH}	r_{O-O}	θ_{OHO}	E_d H_2O-H_2O	r_{O-H}	θ_{HOH}	E_d H_2O-H^+	r_{Oa-H}/r_{Ob-H}	θ_{OHO}	E_d $H_2O-H_3O^+$
PM3[a]	0.95	108	2.77	177	15	0.98	109	590	1.01/1.66	1.47	99
PM3−SSP1[b]	0.97	104	2.74	178	19	1.00	107	638	1.16/1.16	180	136
theor.	0.958[e]	104.4[e]	2.91[f]	172[f]	21[f,d]	0.976[e]	112[e]	685[e,c]	1.20/1.20[g]	173[g]	144[g,d]
expt.	0.957[h]	104.5[h]	2.98[i]	∼180[i]	23[j,d]	0.976[k]	111[k]	694[l,c]			13[m,c]

[a] Original PM3 parameters. [b] PM3 with system specific parameters, see text. [c] Bond dissociation energy (D_0). [d] Classical dissociation energy (D_e) at 0 K. [e] Peterson et al.[51] [f] Hodges et al.[52] [g] Xie et al.[53] [h] Benedict et al.[54] [i] Odutola and Dyke.[55] [j] Curtiss et al.[56] [k] Sears et al.[57] [l] Ng et al.[58] [m] Dalleska et al.[59]

the reaction path CH4 + Cl → CH_3 + HCl and obtained a good PES on, and even off, this path for a wide range of energies. These studies indicate that MNDO-type methods[43] have an inherent ability to provide an accurate description of chemical reactions, if the parameters are modified for the system being studied.

Table 1 compares structural and energetic properties of small H_2O systems obtained from PM3 calculations[60] with theoretical and experimental data. Two major deficiencies of PM3 are the underestimation of the H_2O proton affinity and an incorrect description of the $H_5O_2^+$ ion. Ab initio calculations of $H_5O_2^+$ suggest a global C2 minimum[53] with a very flat, single-well PES for moving the central proton between the oxygen atoms.[61] The PM3 method predicts a strongly asymmetric $H_3O^+-H_2O$ structure, with a barrier of 21 kJ/mol for proton-transfer between the oxygens. Only a shallow local minimum, 18 kJ/mol above the most stable structure, is encountered when the proton is located midway between the oxygens. The PM3 H_2O-H_2O dissociation energy of 15 kJ/mol is slightly lower than ab initio and experimental values of around 21 kJ/mol (see Table 1). The equilibrium O−O distance in $(H_2O)_2$, which is 2.77 Å in PM3, is substantially shorter than experimental and ab initio values (see Table 1) but close to the 2.75 Å given by the TIP4P model. For larger clusters, which is a more relevant comparison for condensed phase simulations, the agreement between PM3 and ab initio values is much better.[62]

To correct the PM3 deficiencies, we have scaled the magnitude of the Gaussian correction functions (GCFs) (attempts to adjust the other PM3 parameters did not give satisfactory results). These GCFs are purely empirical and were originally introduced in the semiempirical methods to fine-tune the balance between repulsive and attractive components of the core−core interaction.[42] It has recently been shown that these GCFs can give rise to spurious oscillations in PM3 PESs.[63] We used a scaling factor of 0.45 for the hydrogen and oxygen GCFs which, in the notation of ref 38, is equivalent to multiplying α_{1O}, α_{2O}, α_{1H}, and α_{2H} with 0.45. All other PM3 parameters were left unchanged. The modified parameter set, which is denoted PM3-SSP1, reproduces the MP2 proton-transfer barrier of 32.8 kJ/mol in $H_5O_2^+$, at an O−O distance of 2.80 Å, as calculated by Ojamäe et al.[61] As shown in Table 1, the PM3-SSP1 $H_5O_2^+$ has a symmetric structure and a much improved $H_2O-H_3O^+$ dissociation energy. The proton affinity of H_2O improves significantly, as does the H_2O-H_2O dissociation energy. Due to the reduction of the GCFs, the spurious minimum in the H_2O-H_2O PES shown in ref 63 disappears. Also, while the original PM3 model predicts one "bifurcated" hydrogen bond in the cyclic structures of $(H_2O)_3$ and $(H_2O)_4$, PM3-SSP1 gives the correct near-linear hydrogen bonding.[52]

The interaction between HCl and H_2O was investigated by comparing PM3 data of small HCl$(H_2O)n$ clusters with theoretical results in the literature.[39,40,64,65] Figure 1 shows some properties of $HCl(H_2O)_{n=0-4}$ clusters. For n larger than 2 only the ring-shaped isomers are shown (see Figure 2a for $n = 4$). The MP2 calculations by Packer and Clary[39] and the B3LYP study of Xie et al.[65] predict a large increase in the HCl bond length, $r_{Cl-H'}$, together with a strong reduction in the H′−O distance,[66] $r_{H'-O}$, with increasing solvation. This is shown in panels (a) and (b) of Figure 1. The PM3 method predicts a far weaker dependence of $r_{Cl-H'}$ and $r_{H'-O}$ on cluster size and, in particular, the HCl bond length does not change when going from $n = 2$ to 4. PM3-SSP1 gives a slight increase when going from $n = 2$ to 4, but the HCl bond length is underestimated. To correct for this, the magnitude of the chlorine GCFs was scaled by a factor of 0.5, and the resulting parameter set (including the SSP1 adjustments) is denoted PM3-SSP2. The resulting HCl bond lengths now follow the ab initio data closely for $n = 0$ to 2. For $n = 3$ there exists a local minimum 1.4 kJ/mol above the equilibrium structure, in which HCl is

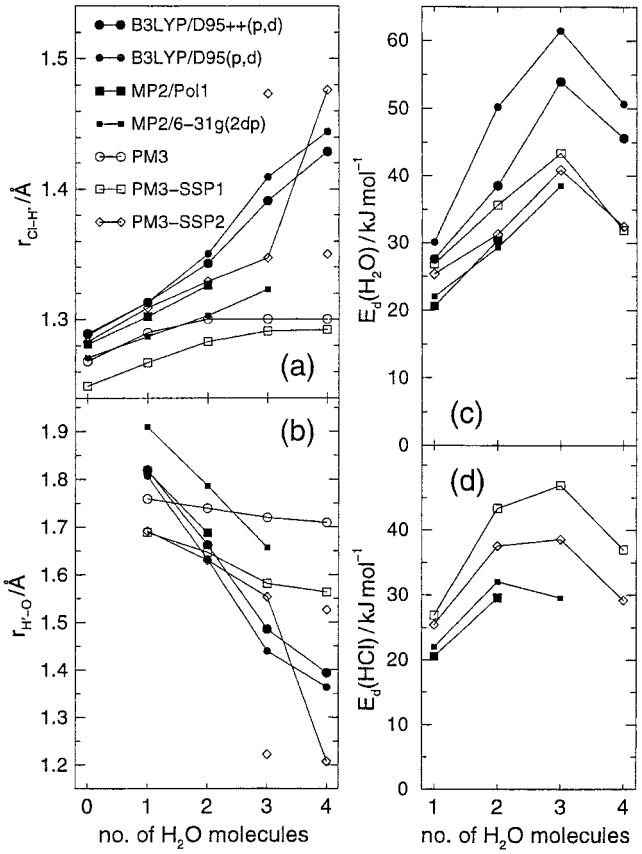

Figure 1. Bond lengths (panels a, b) and dissociation energies (panels c, d) for ring-shaped $HCl(H_2O)_{n=0-4}$ clusters (see text). The results from three different PM3 parameter sets are compared with MP2 calculations of Packer and Clary,[39] and with B3LYP calculations of Schaefer and co-workers.[65] The dissociation energies refer to the processes HCl-$(H_2O)_n$ → $HCl(H_2O)_{n-1}$ + H_2O (panel c) and $HCl(H_2O)_n$ → HCl + $(H_2O)_n$ (panel d), and the ab initio energies do not include zero point energy corrections.

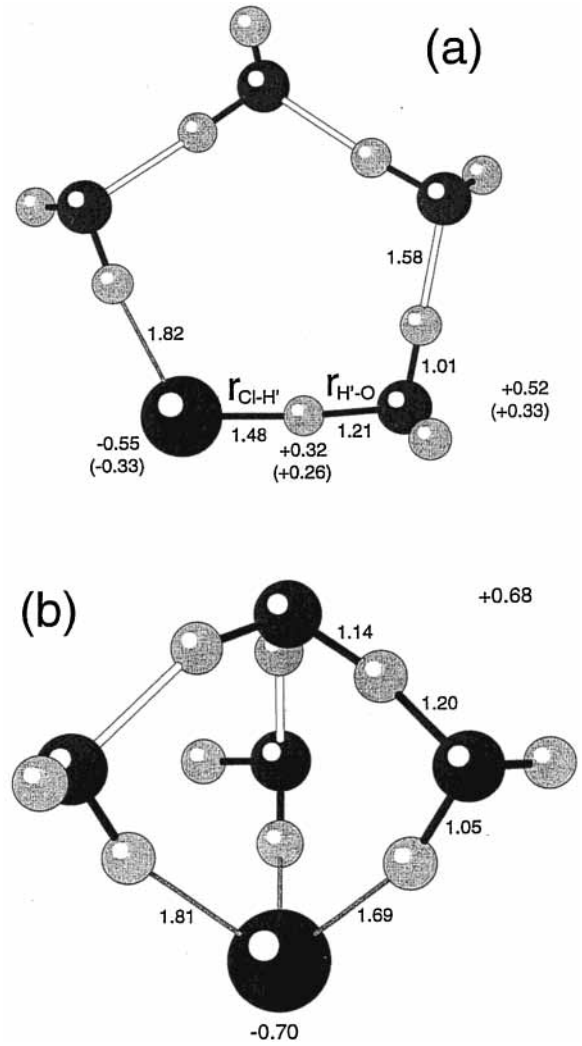

Figure 2. Optimized PM3-SSP2 structures of $HCl(H_2O)_4$. A few bond lengths (Å) and atomic partial charges (see text) are shown. The ring structure (panel a) is 18 kJ/mol above the most stable structure found (panel b). The values within parentheses in panel (a) refer to a nearly degenerate molecular HCl structure (see text). The hydrogens are light gray, the oxygens dark gray, and chlorine black. Covalent bonds are shown as solid lines and hydrogen bonds as open lines.

dissociated, and for $n = 4$ the dissociated structure (shown in Figure 2a) is more stable by 0.3 kJ/mol than the associated structure. These nearly degenerate geometries are included in Figure 1a,b. The $H_2O-HCl(H_2O)_{n-1}$ (panel c) and $HCl-(H_2O)_n$ (panel d) dissociation energies, E_d, for PM3-SSP2 agree well with MP2 values.[39]

In addition to the two near-degenerate ring structures obtained from PM3-SSP2, a third noncyclic minimum was located. Figure 2 shows the dissociated ring structure (panel a) and the noncyclic structure (panel b). The noncyclic structure is the lowest energy structure we were able to locate and is 18 kJ/mol below the structure in panel a. Relevant bond lengths and partial atomic charges are given in the figure. The ring structure is partially ionized, with the chlorine charge of −0.55 being nearly compensated for by the atomic charges on the neighboring H_3O unit, which sum to +0.52. The degree of ionization is even stronger, although not complete, for the geometry shown in panel b. The chlorine charge is −0.70 and the sum of atomic charges on the H_5O_2 unit in the upper right part of the panel is +0.68. Although the charges of the ions in these HCl dissociated structures are less than unity, we will refer to HCl as ionized when the bond length exceeds 1.45 Å (this criterion is based on the simulation results discussed later). We also located a bipyramidal $Cl^-(H_2O)_3H_3O^+$ C_3 local minimum 1.2 kJ/mol above the structure in panel b. In ref 65, the ring structure was found to be 2.9 kJ/mol (13 kJ/mol with the smaller basis set, see Figure 1) above the bipyramid, while PM3-SSP2 yields 17 kJ/mol. Single point QCISD(T) calculations by Bachelo et al.[40] predict this difference to be 4.3 kJ/mol. The original PM3, on the other hand, places the associated ring structure 30 kJ/mol below the double ionic bipyramid. Planas et al. carried out BLYP/TZ94+P calculations on the bipyramid $HCl(H_2O)_3H_2O$ cluster and found that it undergoes barrierless ionization to the $Cl^-(H_2O)_3H_3O^+$ double ionic form via a concerted proton transfer. A similar barrierless ionization, leading to the structure in Figure 2b, is found with the PM3-SSP2 parameter set, which was used in the current study.

2.2. MM and QM/MM Interactions. The molecular mechanics (MM) interactions were described by the empirical TIP4P H_2O model.[33] Point charges $q_H = +0.52$ are placed on the hydrogens and $q_\delta = -1.04$ is placed on a "δ-site" along the HOH bisector, and a Lennard-Jones (LJ) 12−6 term,

$$V_{LJ}(r) = 4\epsilon\left[\left(\frac{\sigma}{r}\right)^{12} - \left(\frac{\sigma}{r}\right)^{6}\right] \tag{3}$$

is centered on the oxygen (r is the O−O distance). The LJ parameters are $\epsilon_{TIP4P} = 0.6487$ kJ/mol and $\sigma_{TIP4P} = 3.154$ Å. The oxygen site has thus zero charge and the hydrogens have no LJ interaction terms. This is one of the most commonly used potentials for water and has been applied in a number of ice surface simulations.[11−14,19−21,23,24,67,68]

The total potential energy of the system can be written as

$$E_{pot} = E_{QM} + E_{MM} + E_{QM/MM} \tag{4}$$

where E_{QM} and E_{MM} are the energies of the QM and MM regions, respectively, and $E_{QM/MM}$ is the interaction energy between these two subsystems. The last term in eq 4 usually consists of electrostatic and van der Waals (vdW) interactions

$$E_{QM/MM} = E_{el} + E_{vdW} \tag{5}$$

The first term in eq 5 includes electrostatic and polarization interactions, and the second term accounts for dispersive attraction and Pauli repulsion and is expressed as a pairwise summation over atom−atom interactions. We have adopted the definition of E_{el} proposed and applied by Cummins and Gready.[69−71] An unscreened Coulomb potential for the interaction between an MM point charge and the QM electron distribution is used, the latter represented by the same multipole expansion used in the QM method. Polarization of the QM electron distribution by the MM charges is incorporated into the SCF procedure by modifying the Fock matrix elements with terms that account for the external MM charges.[69,70] This approach can be expected to be valid if the overlap between the MM and QM charge densities is small, i.e., at sufficiently large interatomic separations. In ref 69 it was shown that using this definition to calculate the molecular electrostatic potential reproduces the exact semiempirical dipole moment of a molecule, even if the potential was probed at distances comparable to atomic vdW radii from the molecule.

While most previous QM/MM simulations of aqueous phase processes have usually ascribed a secondary role to the solvent and included it only in the MM region,[47,70,71] we will use a QM region with up to 24 water molecules. The advantage of this approach, in contrast to using, for example, only one QM water,[32] is that no stringent assumptions have to be made

TABLE 2: Equilibrium Properties of Small H_2O/HCl Systems (bond lengths (r) in Ångström, angles (θ) in degrees, dissociation energies (E_d) in kJ/mol)

	H_2O-H_2O			$H_3O^+-H_2O$			$HCl-H_2O$			$Cl^-(H_2O)_n$		
	r_{O-O}	θ_{OHO}	E_d	r_{O-O}	θ_{OHO}	E_d	r_{Cl-H}	r_{H-O}	E_d	r_{Cl-H}	θ_{ClHO}	E_d
PM3-SSP2[a]	2.74	178	19	2.32	180	136	1.31	1.69	25	1.77	168	71
PM3-SSP2[a]/TIP4P	2.74[b] 2.73[c]	178[b] 171[c]	24[b] 19[c]	2.46	174	109	1.30	1.69	21	2.00	164	70
theor.	2.91[d]	172[d]	21[d]	1.20/1.20[d]	173[d]	140[d]	1.30[g]	1.82[g]	21[g,e]	2.12[h]	168[h]	63[h,e]
expt.	2.98[d]	~180[d]	23[d]			130[d]						59[i,f]

[a] PM3 with system specific parameters, see text. [b] H_2O(TIP4P) hydrogen donor. [c] H_2O(PM3-SSP2) hydrogen donor. [d] See Table 1. [e] Classical dissociation energy at 0 K. [f] Bond dissociation energy. [g] Packer and Clary (MP2/Pol1).[39] [h] Xantheas.[72] [i] Keesee and Castleman.[73]

regarding what reaction path will be explored by the system. In our case, this means that reaction 2 can in principle involve any of the water molecules in the QM region, by a mechanism that does not need to be predefined. Another benefit, which arises when the reaction occurs in the central part of the QM system, is that polarization of molecules within the first solvation is described completely within the QM framework. Since HCl is surrounded by a shell of water molecules, all within the QM region, the most important QM/MM interactions are the H_2O-H_2O hydrogen bonds. As found by, for example, Field et al.,[26] this interaction can be substantially different depending on whether the QM or MM H_2O acts as hydrogen donor. Indeed, simply placing a single LJ term on the QM H_2O oxygen, with TIP4P parameters, yields H_2O-H_2O dissociation energies of 27 (MM donor) and 16 kJ/mol (QM donor). The LJ parameters on the QM oxygens were therefore set to $\epsilon_O = \epsilon_{TIP4P}$ and $\sigma_O = 2.95$ Å (the arithmetic mean of σ_O and σ_{TIP4P} were used when evaluating E_{vdW}). E_{vdW} was furthermore supplemented with a repulsive r^{-8} potential

$$V_8(r) = r\epsilon_8\left(\frac{\sigma}{r}\right)^8 \tag{6}$$

acting between the QM oxygens and the TIP4P hydrogens, with parameters $\epsilon_{8,O} = 0.42$ kJ/mol and $\sigma_{8,O} = 2.1$ Å, thus accounting for part of the Pauli repulsion. The resulting H_2O(QM)$-H_2O$-(TIP4P) equilibrium properties are given in Table 2. The two cases where the MM and QM molecules act as hydrogen donor, respectively, have similar dissociation energies both lying between those predicted by PM3-SSP2 and TIP4P. These parameters also give a reasonable description of the H_3O^+-(QM)$-H_2O$(TIP4P) system. E_{vdW} also includes a repulsion acting between the QM chlorine and the TIP4P hydrogens, according to eq 6, with parameters $\epsilon_{8,Cl} = 0.42$ kJ/mol and $\sigma_{8,Cl} = 2.6$ Å. Table 2 shows that equilibrium properties of the HCl-(QM)$-H_2O$(TIP4P) and Cl^-(QM)$-H_2O$(TIP4P) systems are well described.

2.3. MD Simulations. Born−Oppenheimer molecular dynamics simulations[28] were carried out with the MOPS suite of programs.[37] The classical equations of motion for the atoms in the QM region were solved with the Verlet leapfrog algorithm.[74] The forces were obtained at each time step from converged semiempirical molecular orbital calculations, with the self-consistent field (SCF) convergence criterion set to 4×10^{-12} kJ/mol. The procedure for treating the MM part of the basal ice Ih surface, consisting of all but the 12 or 24 H_2O molecules which constituted the QM region, is detailed in ref 23. Briefly, the complete (QM + MM) surface consists of a $27 \times 31 \times 29$ Å^3 slab of 768 molecules arranged in eight bilayers,[75] with periodic boundary conditions in the surface plane (for the MM molecules) and the molecules in the bottom two bilayers held fixed. Integration of the rigid TIP4P molecules was performed with an implicit quaternion-based Verlet leapfrog algorithm.[76] To model the flux of energy in to and out of the ice slab, it was coupled to a Langevin heat bath by applying local friction and stochastic forces to the molecules in the sixth bilayer.[77,78] The MOPS code was modified to handle the integration of rigid bodies and to include the coupling to the heat bath. The interactions in the MM region were truncated at 10 Å and the QM/MM interactions at 12.5 Å.

Trajectories were typically propagated for 100 ps, using a time step of 1 fs. The $(H_2O)_8$ cluster and ice surfaces were thermalized for at least 30 ps by applying the thermostat of Berendsen et al.,[79] and the final configuration was used in the HCl simulations. The HCl molecule was randomly rotated and initialized with zero vibration and rotation, and the initial velocity was set to 300 m/s, corresponding to a kinetic energy of 1.6 kJ/mol. The HCl was either placed 12 Å from the randomly rotated cluster and impacted head-on, or placed 15 Å above the center of the QM region with the velocity in the surface normal (z) direction. The initial velocities of the atoms and rigid molecules in the cluster or surface were sampled from a thermal distribution. Each HCl + $(H_2O)_8$ trajectory was performed at constant energy, with no overall rotation of the system, while the HCl + ice surface trajectories included coupling to a heat bath as described above. Propagating one HCl + $(H_2O)_8$ trajectory for 100 ps requires approximately one CPU hour on a 195 MHz R10000 processor, and an ice surface with 12 QM water molecules takes 43 h.

3. Results

3.1. HCl + $(H_2O)_8$. The $(H_2O)_8$ cubic cluster was found to be stable, i.e., the hydrogen bond network does not reconstruct, for at least 100 ps, even at temperatures as high as 200 K. This suggests that the cubic geometry is not a high-energy metastable structure.[80] The dissociation energy of the cluster, defined as the energy difference between the optimized $(H_2O)_8$ system and eight noninteracting water molecules, is 271 kJ/mol. This is similar to the energies obtained from PM3, ab initio and empirical potentials.[46]

Figure 3 shows snapshots from an HCl + $(H_2O)_8$ trajectory, with an initial cluster temperature of 100 K. The impinging HCl molecule rapidly hydrogen bonds to a dangling oxygen. The structure at 11.95 ps is typical for HCl adsorbed on the 100 K cluster. After 12.80 ps the Cl atom has come into contact with a dangling hydrogen, and 0.2 ps later (13.00 ps) the $(H_2O)_8$ cube has opened up with the HCl being incorporated in the hydrogen bond network. The subsequent HCl ionization (13.15 ps) occurs rapidly and is followed by an additional H_2O-H_2O hydrogen bond breaking and an H_2O-Cl^- bond being formed (13.45 ps). This enhances the solvation of the chloride ion. Although rearrangements in the hydrogen bond network over the remainder of the trajectory are seemingly small, they have a substantial impact on the energetics (discussed below). The final structure is nearly cubic, except that two of the six faces consist of five-membered rings. The chloride ion is in direct contact with an H_3O^+ ion, which makes frequent transformations to an $H_5O_2^+$ structure.

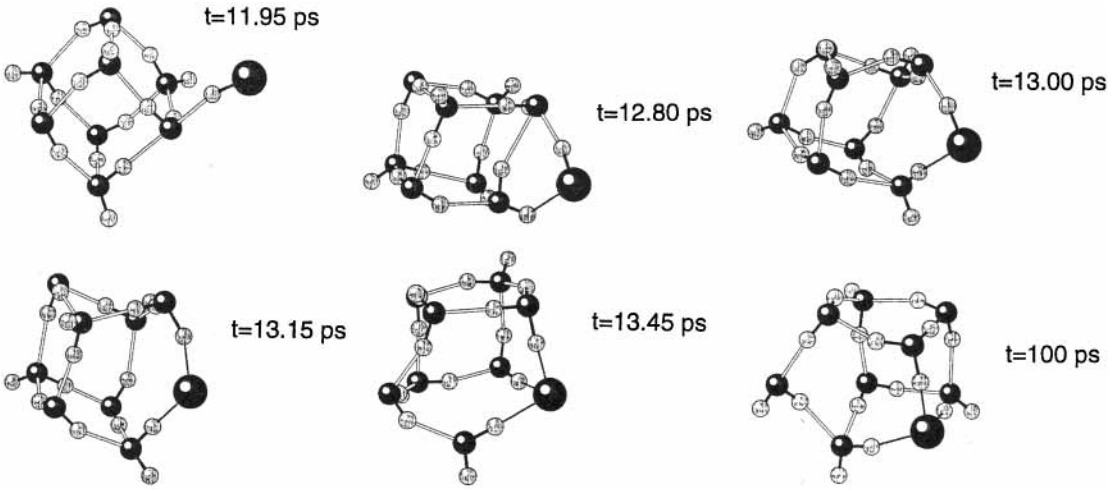

Figure 3. Snapshots from a HCl + $(H_2O)_8$ trajectory, with an initial cluster temperature of 100 K. Shading of atoms as in Figure 2.

The HCl ionization, which occurs between 13.00 and 13.15 ps, can be compared with the HCl$(H_2O)_4$ ring structure in Figure 2a, which has both a molecular and ionized form almost degenerate in energy. The major difference is that, in the HCl-$(H_2O)_8$ cluster, the water molecule accepting the HCl proton donates both its hydrogens to neighboring water molecules, instead of only one. This leads to optimal solvation for the product H_3O^+ ion.[83] A corresponding enhanced solvation of the water molecule binding to Cl is also apparent. These two factors work in favor of HCl ionization.

Figure 4 compares data from the trajectory in Figure 3 with one in which HCl does not ionize.[84] The distance between Cl and the cluster center of mass (CM), r_{Cl-CM}, the HCl bond length, $r_{Cl-H'}$, and the minimum distance of the HCl hydrogen[66] to an oxygen, $r_{H'-O}$, are shown as a function of time in panels (a) to (c). These panels clearly show the HCl ionization at 13 ps seen in Figure 3. The Cl−H′ and H′−O distances show that after 13 ps there is no recurrence to molecular HCl. Also, the constant value of $r_{Cl-H'}$ (∼1.7 Å) indicates that there is no proton migration. The bottom two panels show the temperature, T, and potential energy, E_p, of the cluster, which are mirror images of each other since total energy is conserved. For both trajectories the initial temperature is 100 K, but due to the HCl−$(H_2O)_8$ attractive interaction it rapidly rises to −140 K. The temperature of the trajectory in which the HCl does not ionize fluctuates around this value over the 100 ps simulation. In the ionizing trajectory, on the other hand, a substantial amount of energy is released, and after 100 ps the temperature has risen to −200 K. Interestingly, the actual ionization step at 13 ps is not connected to a direct release of energy, but the rise in temperature and fall in potential energy occur gradually over the 100 ps trajectory. The differences between the cluster structures at 13.45 and 100 ps in Figure 3 account for this behavior. A close inspection of these two geometries reveals differences in the hydrogen bonding, and thus polarization, of the two water molecules that bind to the chloride ion and the two water molecules that bind to the hydronium ion.

A total of 19 HCl + $(H_2O)_8$ 100 ps trajectories were simulated for each of the temperatures 100, 150, and 200 K. One of the trajectories at 100 K resulted in HCl ionization within 100 ps, six at 150 K and eleven at 200 K. Although there are too few trajectories for statistical analysis of the ionization rate, we can conclude that HCl ionization in the $(H_2O)_8$ cluster is an activated and thermodynamically spontaneous process. At the two lowest temperatures the ionization mechanism is appropriately described by Figure 3. At an initial cluster temperature of 200 K, which due to the HCl adsorption rises to ∼250 K, ionization is sometimes initialized by cluster melting. In these cases the $(H_2O)_8$ cube can open up in many different ways and subsequently find a configuration which favors HCl ionization. Two

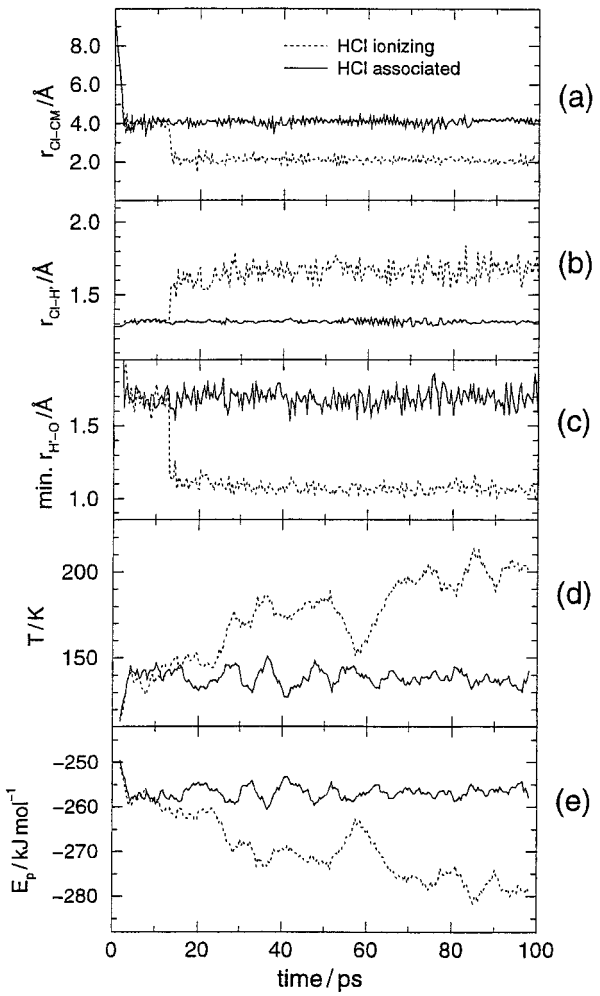

Figure 4. Time-evolution of a few properties of the ionizing HCl + $(H_2O)_8$ trajectory in Figure 3 and one in which HCl remains molecular, both clusters initially at 100 K. The distances in panels a−c are defined in the text. The temperature (panel d) is obtained from the kinetic energy via the classical equipartition theorem, and the potential energy (panel e) is measured relative to that of the isolated molecules HCl + $8H_2O$. The curves in (d) and (e) are 10-point running averages of instantaneous values.

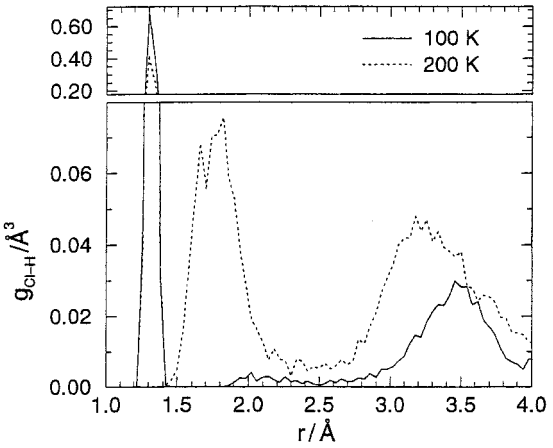

Figure 5. Radial Cl−H distribution function from the HCl + $(H_2O)_8$ simulations, with the initial cluster temperatures 100 and 200 K. Each curve represents an average over fourteen 100 ps trajectories.

of the 57 trajectories result in scattering of the HCl from the cluster. In these runs the chlorine end of the HCl impacts with the cluster, either hitting a dangling oxygen and scattering directly, or forming a weak, short-lived bond with a dangling hydrogen.

Figure 5 shows the radial Cl−H distribution function, g_{Cl-H}, normalized so that

$$N_{Cl-H}(r) = r\pi \int_0^r r'^2{}_{Cl-H}(r')\, dr' \qquad (7)$$

gives the average number of hydrogens within a distance r from Cl, and $N_{Cl-H}(\infty) = 17$. At 100 K almost all HCl is molecular−the peak at −1.3 Å gives the average HCl bond length−while at 200 K a peak appears between 1.5 and 2.1 Å, which is due to the chloride ion binding to one H_3O^+ hydrogen and 1−2 additional H_2O hydrogens. Since HCl ionization in the $(H_2O)_8$ cluster is an activated process, these distributions depend on the length of the simulation. For sufficiently long times the molecular HCl peak at 1.3 Å will be far less intense than the ionized HCl peak at both temperatures.

3.2. HCl + Ice. The top bilayer of the ideal basal plane of ice Ih consists of puckered hexagonal rings (chairs), with every second molecule lying in the upper monolayer. While the top monolayer molecules have 3-fold coordination, making their interaction with adsorbates particularly strong, all molecules below the top monolayer have 4-fold coordination. The QM region in the ice surfaces consisted of 12 or 24 water molecules in the top bilayer, with a hexagonal ring in the center. Four different sites were studied and classified according to the orientations of the three top monolayer molecules in the central hexagon. The number of free hydrogens (oxygens) in the central hexagon were 1(2) (surface I), 2(1) (surface II), 3(0) (surface III) and 0(3) (surface IV).

The PM3-SSP2 binding energy of HCl to the ice surface was determined by running damped trajectories, in which HCl was initially directed to the central hexagon of these four surfaces and the kinetic energy of the system gradually removed. The potential energy of the damped system was subtracted from that of HCl and ice surface optimized separately. For HCl on surface I, with the optimized geometry shown in Figure 6a, the binding energy is 43 kJ/mol. The Cl−H′ bond length is 1.34 Å and the H′−O distance[66] is 1.60 Å. These values lie between those found for the $HCl(H_2O)_2$ and $HCl(H_2O)_3$ clusters, which is reasonable since the HCl forms a strained ring with three water molecules. As seen in the figure, distortions from the ideal lattice structure are small.

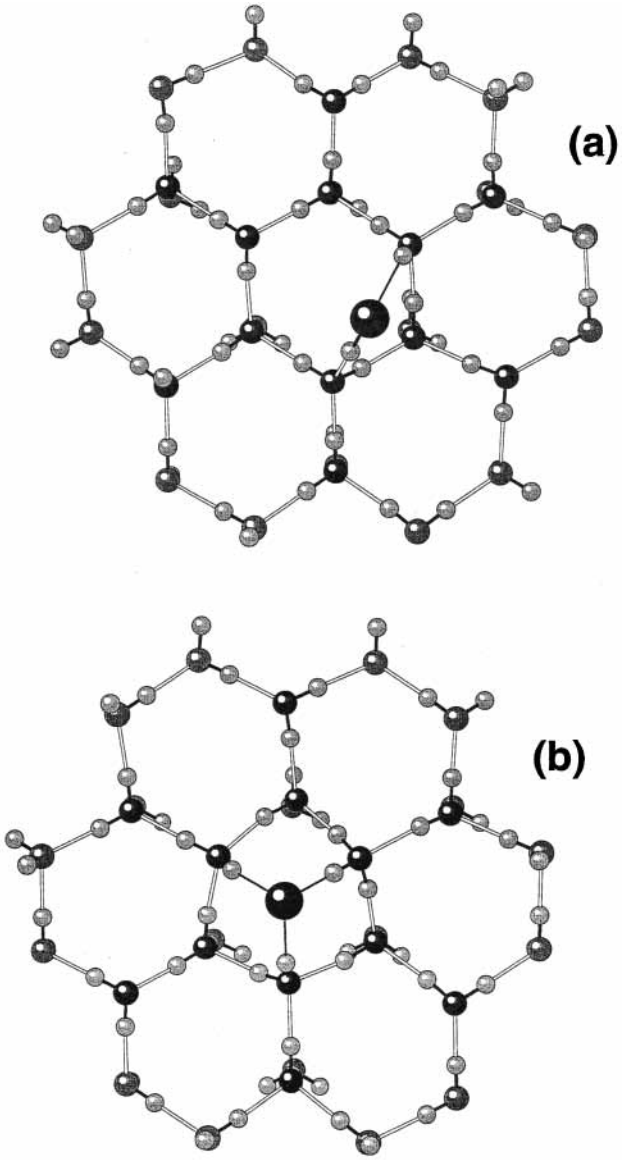

Figure 6. Optimized geometries for HCl at two different sites of the basal ice Ih surface. When the central hexagon contains one dangling hydrogen, HCl adsorbs molecularly (panel a), and when it has two dangling hydrogens HCl ionizes (panel b). HCl and the closest 12 water molecules in the surface are described by PM3-SSP2 (see text) and have the same shading as in Figure 2. The remainder of the ice surface is described by the TIP4P model, with oxygens shaded gray (only 18 TIP4P molecules are shown).

The damped trajectory of HCl on surface II leads directly to HCl ionization, and involves a small or zero barrier. The ionized structure is shown in Figure 6b. The Cl−H′ and H′−O distances are 1.61 and 1.10 Å, respectively, the latter value being slightly larger than an unperturbed H_3O^+ intramolecular bond. The binding energy, including the contribution from the ionization, is 64 kJ/mol. As seen in the figure, there is extensive structural relaxation of the ice lattice, with pronounced contraction of the central hexagon. When the surface is kept frozen in its ideal structure, HCl adsorbs molecularly with a binding energy of 41 kJ/mol. Surface relaxation is thus crucial for ionization. These binding energies are compared with literature data in Table 3, and will be discussed in the next section.

In optimizations on surfaces III and IV, the HCl molecule flipped from the central hexagon to a nearby hexagon with two free hydrogens, i.e., a type II site. The flipping was simulated in order to ascertain the flipping dynamics. On surface IV, the

TABLE 3: HCl Desorption Energies, E_{des}, (kJ/mol) with Ice Surfaces

method	surface	*T*/K	HCl assignment	E_{des}
QM/MM[a]	surface I	0	molecular	43
QM/MM[a]	surface II	0	ionized	64
QM/MM[a]	surface II[i]	0	molecular	41
Ab initio[b]	periodic[i] (P-chair)	0	molecular	33
Anal. PES[c]	TIP4P	0[i] 190	molecular[j]	22−29 19[k]
Anal. PES[d]	TIP4P	190	molecular	25−33[k]
adsorption-model[e]	ice		ionized	≥75[l]
kinetics-model[f]	ice	100−125	molecular	28 ± 2
expt.[g]	hexahydrate	120−150	molecular	33 ± 5
expt.[h]	liquid water	298	ionized	74.8[l]

[a] This work, PM3-SSP2. [b] Bussolin et al.[34] [c] Kroes and Clary.[11] [d] Clary and Wang.[13] [e] Tabazadeh and Turco.[85] [f] Isakson and Sitz.[16] [g] Graham and Roberts.[86] [h] Reference 87. [i] Rigid and ideal surface. [j] Rigid HCl. [k] Desorption energy calculated from the average potential energy of HCl. [l] (Negative value of) Enthalpy of adsorption/solution.

HCl flips out of the central hexagon in 10 out of 10 simulations, both at 0 and 180 K. For surface III it flips in 5 out of 10 and 3 out of 10 trajectories at 0 and 180 K, respectively. Type III and IV sites are relatively rare on the ideal ice Ih basal plane.[88] We conclude that the large majority of HCl molecules impinging randomly on an ideal ice Ih basal surface will rapidly attach to type I and type II hexagons, and only these sites will be considered below.

Surfaces I and II were thermalized at 150 K and, in agreement with our earlier studies of "pure" TIP4P surfaces,[23,24] the hexagonal structure of all bilayers was conserved over the simulation times studied here. The dynamics of HCl colliding with surface I shows features similar to the behavior described for type III and IV sites. While HCl adsorbs initially in the configuration shown in Figure 6a, the bond between Cl and the dangling hydrogen is weak and breaks quite rapidly at 150 K. The HCl then has the possibility of flipping to a nearby hexagon. This mechanism is illustrated in Figure 7. Note that during this process the strong $ClH-OH_2$ hydrogen bond is preserved. There are, therefore, two possible hexagons to which HCl can flip. In all of the 5 simulations at 150 K, flipping occurs within 30 ps after HCl has impacted on the surface. Since HCl always flips to a type II site, we will focus the discussion on this site. At this site, HCl ionizes directly on impact as it did in the damped trajectory simulations. Furthermore, hydrogen chlorine remains in the ionized form throughout the 100 ps simulation time for all five trajectories. The chloride ion also remains in the middle of the central hexagon, as shown in Figure 6b.

At 180 K, which is close to the lower temperature limit of the polar stratosphere, the mobility of the top bilayer molecules increases.[23,24,67] To maintain a primary solvation of HCl by QM water molecules during the simulation, the QM region was increased to 24 molecules, i.e., all of the top bilayer molecules shown in Figure 6b. Figure 8 shows time-dependent results for HCl interacting with surface II. The higher temperature leads to large fluctuations compared to the cluster trajectory results obtained at 100 K (see Figure 4). In the first simulation, HCl ionizes after ∼40 ps, as seen from the Cl−H′ (panel b) and H′−O (panel c) distances,[66] although large fluctuations are also apparent prior to this. The point of HCl ionization also coincides with a slight penetration of Cl into the surface as shown by its *z*-coordinate, *z*Cl (panel a). Examination of all 10 trajectories run under these conditions reveals that this is a general trend and is a result of the product chloride ion acquiring a higher degree of solvation. In the second simulation, HCl remains molecular over most of the trajectory, although it does make

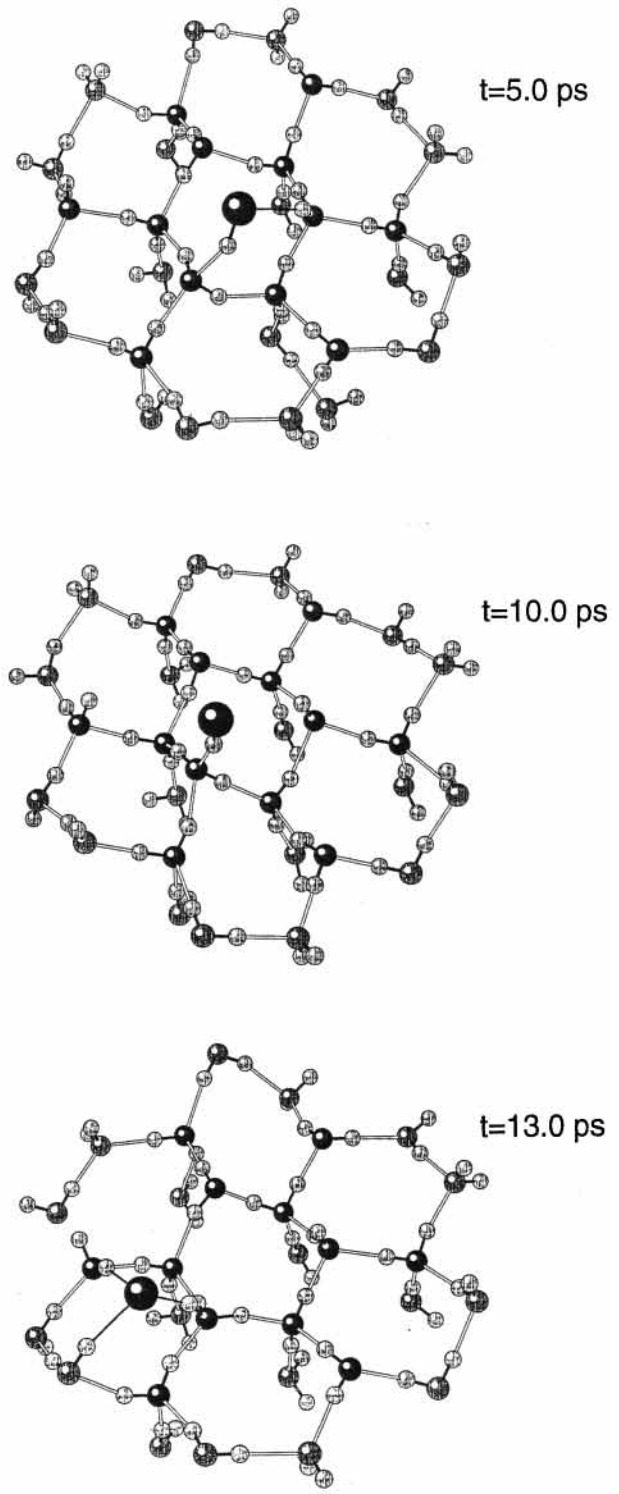

Figure 7. Snapshots from a simulation of HCl on an ice surface at 150 K. The frames show the flipping motion of HCl from the central surface hexagon, containing one free hydrogen, to a neighboring hexagon with two free hydrogens where HCl rapidly ionizes. Shading of atoms as in Figure 6.

both rapid and extensive excursions into the ionized state. The third simulation displays rapid ionization, followed by a dramatic increase in the Cl−H′ distance at ∼60 ps, eventually increasing to more than 4 Å (not shown). The H′−O distance simultaneously drops slightly below 1.0 Å, typical of the OH bond length in H_2O. Analysis of the trajectory reveals that this is due to a Grotthuss proton hopping event,[89] moving the H_3O^+ structure from one side of the hexagon to the opposite side.

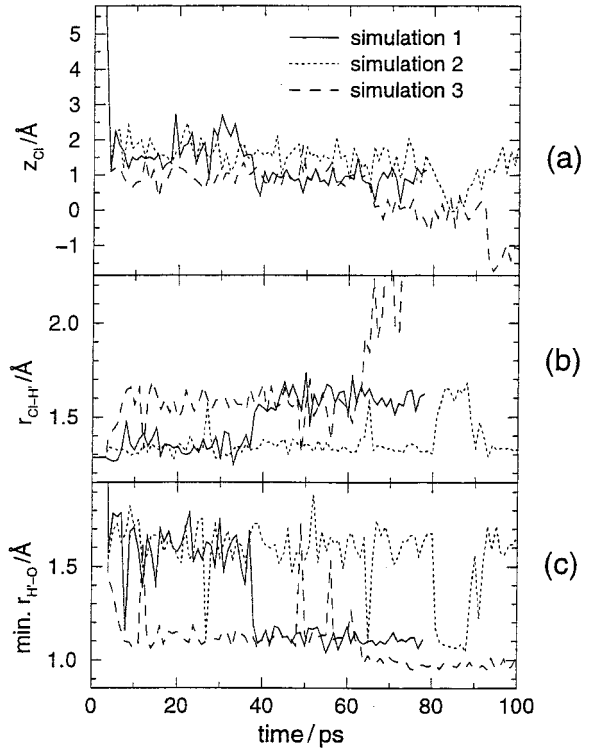

Figure 8. Time evolution of a few distances in three different simulations of HCl colliding with an ice surface at 180 K. The different distances are defined in the text, and the oxygens in the top monolayer are located between 1 and 0 Å.

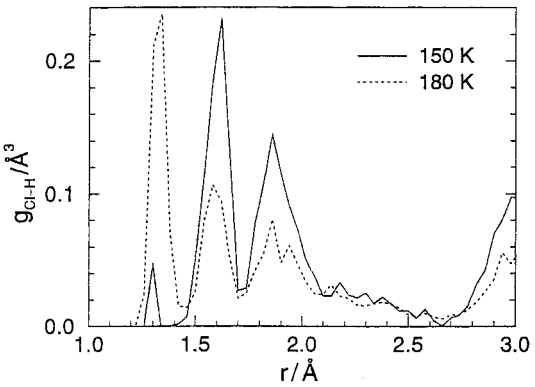

Figure 9. Radial Cl−H distribution function from the HCl + ice surface II simulations at the temperatures 150 and 180 K. The curves represent an average over a total simulation time of 500 ps (150 K) and 770 ps (180 K).

This is followed by a displacement of the chloride ion to a H_2O lattice position in the hexagon. During these two rearrangements the contact ion pair structure is conserved. For HCl collisions with surface II at 180 K, ionization occurs within 70 ps in 6 out of the 10 simulations.

Figure 9 shows the radial Cl−H distribution at 150 and 180 K. As mentioned earlier, HCl ionizes rapidly on surface II at 150 K, which results in a small peak at 1.3 Å due to molecular HCl and a large peak between 1.5 and 1.7 Å originating from the Cl^-−H_3O^+ contact ion pair. At 180 K the molecular HCl peak is much stronger and the contact ion pair peak correspondingly weaker. This is consistent with the data shown in Figure 8b. As observed in previous simulations,[23,24,67] at 180 K the ice surfaces show a tendency for the surface hexagons to reconstruct. For example, in one of the trajectories a dangling hydrogen H_2O in the central hexagon has flipped down to the second monolayer, binding to a molecule in the second bilayer,

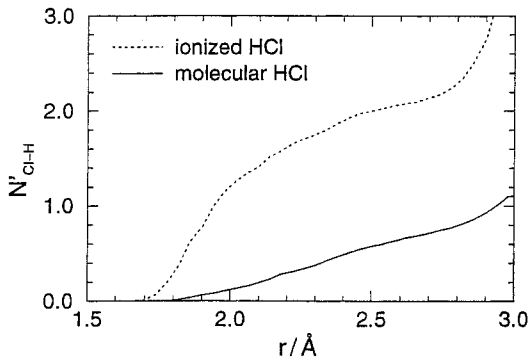

Figure 10. Data from 10 simulations of HCl colliding with an ice surface at 180 K, showing the correlation between the HCl structure, i.e., molecular or ionized, and the number of dangling hydrogens solvating the Cl atom/ion (see text).

thus leaving only one dangling hydrogen in the hexagon. Not all simulations lead directly to ionization at impact, and HCl can display the flipping motion illustrated in Figure 7. When sufficiently solvated HCl may ionize or it may recombine at a later stage. However, when the chloride ion penetrates below the ice surface plane ($z \approx 0$ Å), the ions do not recombine to molecular HCl within the simulation time.

The data shown in Figure 10, which is obtained at 180 K, quantifiy the correlation between the availability of dangling hydrogens at the surface and the tendency for HCl to ionize. On the basis of Figure 9, the shortest Cl−H distance is used to determine if HCl is molecular or ionized. Data shown by the solid and dotted curves in Figure 10 are for the molecular (shortest Cl−H distance less than 1.45 Å) and ionized (shortest Cl−H distance larger than 1.45 Å) structures, respectively. Each distribution, N'_{Cl-H}, gives the average number of hydrogens, not counting the closest one, within a given distance from the Cl. The distributions clearly show that molecular HCl has a small number of additional hydrogens in the vicinity of Cl. Ionized HCl, on the other hand, is correlated with a high abundance of solvating hydrogens, and more than one additional hydrogen is, on average, found within 2.0 Å from the Cl ion.

4. Discussion

Simulations of the HCl−$(H_2O)_8$ cluster collisions showed direct scattering, molecular adsorption, and HCl ionization, and that the latter two reaction channels dominate. Although the number of simulated trajectories is rather limited, there is strong evidence that the ionization rate increases with temperature and HCl ionization in the $(H_2O)_8$ cluster is thus an activated process. None of the trajectories showed association of the ions to molecular HCl, indicating that the ionized structure is stable.

For the HCl−ice surface system we have identified and studied collisions with four different surface hexagon sites. Batista and Jónsson[68] have shown that these sites are important for the binding characteristics of H_2O adsorbed on ice surfaces. Damped trajectory collisions with sites III and IV (3 and 0 dangling hydrogens, respectively) result in flipping to a neighboring site II (2 dangling hydrogens), showing that there is a small or zero barrier to flipping. When the HCl molecule collides with site I (1 dangling hydrogen), one strong (ClH−OH_2) and one weak (HCl−H_2O) hydrogen bond is formed and the HCl becomes trapped on the surface. Collision with site II results in a second weak hydrogen bond being formed, and damped trajectory collisions show rapid ionization over a small or zero barrier. Relaxation of the ice lattice is essential for ionization. The chloride ion moves a short distance into the

surface hexagon, thereby increasing its solvation. None of the trajectories at 150 K show association of the contact ion pair, confirming that it is a stable structure. At 180 K, on the other hand, recombination to the molecular state was observed.

The validity of the results obtained from MD simulations depends, among other things, on the accuracy of the PES. In addition to the direct scattering and trapping channels, the simulations show that HCl can ionize readily on the basal surface of ice Ih. This reaction channel may be of importance, for example, to stratospheric chemistry,[85] and it is important that this reaction path is accurately described by PM3-SSP2 and that it is not sensitive to minor inaccuracies in the PES. As discussed in section 2, we fit the PM3 parameters to ab initio data available for small clusters. In agreement with the B3LYP study of Re et al.,[65] the molecular $HCl(H_2O)_n$ structures are more stable than the ionized structures for $n \leq 3$, and both molecular and ionized structures (similar in energy) are found for $n = 4$. They also found that the ionized structure is the most stable for $n = 5$. Similarly, B3LYP and MP2 results[40] yield near-degenerate minima for both molecular and ionized forms of the $HCl(H_2O)_4$ cluster. Although the ordering of the PM3-SSP2 energies for these structures is different from that of the ab initio energies,[90] these differences are small and are difficult to determine accurately. The calculations in refs 40 and 65 provide support for the low energy ionized $HCl(H_2O)_4$ structure predicted by PM3-SSP2. When mapping out the PES of the bipyramid $HCl-(H_2O)_4$ cluster, which is reminiscent of a type II surface site, Planas et al.[64] found that HCl ionization is barrierless and strongly exothermic. The molecular form of the $HCl(H_2O)_4$ bipyramid is thus a high-energy unstable structure. Efficient HCl ionization on type II surface sites is therefore not surprising, and the present work constitutes an assessment of the influence of the surrounding ice lattice in constraining the geometry of the reaction center. We plan to perform high-level ab initio calculations on the HCl−ice surface system to confirm and quantify the HCl ionization mechanism found on the type II surface.

The sensitivity of HCl ionization on the PM3-SSP2 description was tested by repeating the simulations of HCl impinging on surface II at 150 K, using PM3-SSP1 (which was found to yield only molecular $HCl-(H_2O)_{n=2-4}$ ring structures). Keeping in mind the unrealistically high $HCl-(H_2O)_n$ dissociation energies of PM3-SSP1 (Figure 1), the main difference in the dynamics is that instead of an irreversible ionization there is rapid transfer between ionized and molecular states. This behavior is similar to that found at 180 K with PM3-SSP2, and on time-scales longer than 100 ps solvation of the ion pair configurations would probably increase, thereby increasing the contact ion pair stability.

The conclusions drawn from the MD simulations are not expected to be sensitive to quantum dynamical effects. Agreement between experiments and MD simulations for Ar−ice collisions[25] shows that classical dynamics provides a valid description for Ar−ice collisional energy transfer and trapping. The large Ar mass and flexible molecular ice surface leads to efficient energy transfer. Since the mass of HCl is the same as that of Ar a similar energy transfer mechanism is expected.[17] The larger HCl−ice attraction, compared to that for Ar−ice, leads to a trapping coefficient near unity.[15−17] Although quantum effects, such as tunneling, may affect the $HCl(H_2O)$ and H_2O-H_2O proton transfer rates,[20,91] they are not expected to alter the qualitative transfer mechanisms reported here. As mentioned above, Planas et al.[64] found that HCl ionization in $HCl(H_2O)_4$ is barrierless, and Hynes et al.[19−21] have shown that, when HCl is incorporated in the ice lattice, proton transfer occurs over a small barrier. The barrier for H_2O-H_2O proton transfer depends on the intermolecular separation and relative orientation and vanishes as the O−O distance approaches 2.40 Å.[61] Since H_2O solvent fluctuations are expected to be fairly well described classically, MD simulations should provide valid qualitative mechanistic descriptions of the proton transfer. Previous classical MD studies have led to the same conclusions.[29,92,93]

The current simulations generally agree with the results of earlier MD studies of the HCl−ice system.[11−14,19−21] Robertson and Clary[12] have shown that HCl ionization on an ice surface may be energetically favorable. They did not differentiate between different surface sites, as was done in this work, and did not determine the ionization barrier height. The simulations of Kroes and Clary[11] show that the HCl binds strongly with its hydrogen to a surface H_2O oxygen, which is confirmed by the current work.

The present model showed that relaxation of the ice lattice is essential for HCl ionization on the surface. This may explain the discrepancy between our results and those of Hynes and co-workers,[21] who found that ionized HCl is not thermodynamically stable on the ice surface, since they constrained the surface to its ideal structure. They have also shown[19−21] that a stable contact ion pair is formed when HCl is placed within the ice lattice. When investigating 14 different ionization sites,[20] and including a quantum correction for the change in zero point energy of the transferring proton, they found Gibbs free energy changes for the ionization process ranging from −19 to −40 kJ/mol, with small barriers between 0.8 and 6.7 kJ/mol. The present work compliments these earlier theoretical studies by using a direct approach to investigating HCl trapping and ionization on ice surfaces. No constraints are placed on the reaction center, which represents an important difference to, in particular, ab initio studies.[34,35]

A detailed comparison with measured data on HCl−ice systems is complicated by the much longer time scales probed in experiments, as well as the influence of HCl−HCl interactions. However, the rapid and exothermic HCl ionization observed in the simulations is in general agreement with the efficient HCl uptake of the order of one monolayer obtained from experiments under stratospheric conditions.[6,8,9] Table 3 compares the calculated HCl−ice interaction energies with theoretical and experimental data available in the literature. The value of 41 kJ/mol, obtained with a rigid type II surface, is somewhat higher than the values obtained from the MP2 calculations of Bussolin et al.[34] (33 kJ/mol) and the analytic PES result of Kroes and Clary[11] (29 kJ/mol). This is reasonable since HCl was constrained to be rigid in the latter study. As showed by Clary and co-workers,[11,13] this energy is sensitive to surface defects, and the effective desorption energy at stratospheric temperatures can be substantially lower due to the thermal perturbation of the surface. The 64 kJ/mol desorption energy obtained for ionized HCl at a type II site is close to the estimated adsorption enthalpy from Tabazadeh and Turco[85] ($\geq$75 kJ/mol), which is the result from a model based on uptake measurements at low HCl pressures. It is also close to the solvation enthalpy of HCl in liquid water (74.8 kJ/mol).

The simulations also predict a (metastable) molecularly adsorbed state, whose lifetime depends sensitively on the barrier for HCl to diffuse to a type II site or to gain sufficient solvation for ionization by another mechanism. This picture is in qualitative agreement with the experimental findings of Isakson and Sitz[16] who obtained a desorption energy of 28 kJ/mol and an activation energy of 21 kJ/mol for loss of this state. A

metastable adsorbed state was also observed in the experiments of Delzeit et al.[94] if the temperature was below 60 K. The present results are not consistent with their recent infrared spectroscopy study, indicating that molecularly adsorbed HCl is thermodynamically stable at 125 K at low coverage.[95]

The (essentially) barrierless HCl ionization mechanism revealed by the present calculations requires a surface hexagon with two dangling hydrogens, and might therefore be specific for this type of site. The simulations with surfaces at 180 K, which to some extent reconstruct, and the HCl + $(H_2O)_8$ simulations show that on a time-scale of 100 ps, HCl ionizes readily even if two dangling hydrogens are not available initially. This provides a consistent picture of facile HCl ionization on the ice surface, a behavior which is not sensitive to the precise structure of the ice and which does not require HCl to first become encapsulated by condensing water molecules. Similar ionization mechanisms can therefore be expected to be valid for HCl sticking to the surfaces of amorphous ice, liquid water, and possibly water-rich PSC type I particles.

The structure of HCl-covered ice surfaces, especially the locations of chloride and hydronium ions, controls the mechanisms and thereby the efficiency of subsequent reactions involving, for example, an impinging $ClONO_2$ molecule. A chloride ion occupying a top bilayer hexagon, as in Figure 6b, would provide a nucleophilic site in the interaction with adsorbates. Ion-assisted mechanisms have been proposed by MacTaylor et al.[96] in explaining the observed HCl uptake by $D^+(D_2O)_n$ clusters and in the reaction of $ClONO_2$ on acidic surfaces.[5] HCl molecules binding to chloride ions in the surface may also be the origin of the adsorbed "α-HCl" state observed in the temperature-programmed desorption study of Graham and Roberts.[86] Another important aspect of the ionized HCl structure in Figure 6b is that it depletes the surface of dangling hydrogens, since two dangling H_2O hydrogens and one oxygen in the hexagon become bonded. None of the six neighboring hexagons can provide a subsequent HCl molecule with two dangling hydrogens, which is required for ionization. Assuming that molecularly adsorbed HCl will have a comparatively short surface residence time, this ionization structure sets a limiting coverage of one HCl per three surface hexagons. With the conventional assumption of 1×10^{15} sites/cm^2, this equals 0.33 monolayers, which is in the range of saturation uptake at low HCl partial pressures estimated from experiments.[6,8,9] We note, however, that the precise stability and lifetime of the configuration in Figure 6b is difficult to judge, and that the simulations at 180 K reveal a slight tendency for the chloride ion to descend into the first bilayer to gain enhanced solvation.

As a final comment, we note that a complete and automated reoptimization of all PM3 parameters,[47,49] using a larger reference data set than employed here, appears to have the potential of accurately describing a wide range of aqueous phase reactions. Work in this direction is in progress.

5. Conclusions

We have developed and used coupled QM/MM classical MD code to study the trapping, solvation, and ionization of HCl impinging on the basal plane of ice Ih and a cubic $(H_2O)_8$ cluster. The validity of the semiempirical PM3 method for describing the QM region was critically examined, and a few parameters were tuned to improve the description of important features of the present system. The set of modified parameters that were used for the simulations is called PM3-SSP2. The simulations reveal a mechanism by which HCl can readily ionize on ice surfaces, without the need to be encapsulated in the ice lattice. The possibility of ionization depends critically on the availability of dangling H_2O hydrogens that can solvate the chloride ion and relaxation of the surrounding lattice structure. Thus, an important aspect of the present model is that no geometrical restraints are placed on the reactants, and the full multidimensional PES of the reaction center is extensively explored in the simulations, covering of the order of 106 different configurations.

The present results are in agreement with previous experimental[15−17] and theoretical[11−14] studies which predict a high accommodation coefficient for HCl on clean ice surfaces. They are also consistent with experiments, which yield an uptake on the order of one monolayer under stratospheric conditions,[6,8,9] and measurements which indicate the presence of hydronium ions at the surface also at low temperatures.[6,10,94] The ionization mechanism observed here may be important for the structure and reactivity of HCl-covered ice particles present in the cold polar stratosphere.

Acknowledgment. We are grateful to Drs. Peter Cummins and Jill Gready for providing us with the MOPS code and for valuable discussions. M.S. and J.P. are thankful to the Swedish Natural Science Research Council for financial support, and K.B. is grateful to Adlerbertska Forskningsfonden.

References and Notes

(1) Farman, J. C.; Gardiner, B. G.; Shanklin, J. D. *Nature* **1985**, *315*, 207.

(2) (a) Tolbert, M. A. *Science* **1996**, *272*, 1597. (b) Peter, T. *Annu. Rev. Phys. Chem.* **1997**, *48*, 785. (c) Schreiner, J.; Voigt, C.; Kohlmann, A.; Arnold, F.; Mauersberger K.; Larsen, N. *Science* **1999**, *283*, 968.

(3) Molina, M. J.; Tso, T.-L.; Molina, L. T.; Wang, F. C.-Y. *Science* **1987**, *238*, 1253.

(4) (a) Chu, L. T.; Leu, M.-T.; Keyser, L. F. *J. Phys. Chem.* **1993**, *97*, 12798. (b) Opplinger, R.; Allanic, A.; Rossi, M. J. *J. Phys. Chem. A* **1997**, *101*, 1903.

(5) Horn, A. B.; Sodeau, J. R.; Roddis, T. B.; Williams, N. A. *J. Phys. Chem. A* **1998**, *102*, 6107.

(6) Hanson, D. R.; Ravishankara, A. R. *J. Phys. Chem.* **1992**, *96*, 2682.

(7) McNamara, J. P.; Hillier, I. H. *J. Phys. Chem. A* **1999**, *103*, 7310.

(8) Abbat, J. P. D.; Beyer, K. D.; Fucaloro, A. F.; McMahon, J. R.; Wooldridge, P. J.; Zhang, R.; Molina, M. J. *J. Geophys. Res.* **1992**, *97* D14, 15819.

(9) Chu, L. T.; Leu, M.-T.; Keyser, L. F. *J. Phys. Chem.* **1993**, *97*, 7779.

(10) Horn, A. B.; Chesters, M. A.; McCoustra, M. R. S.; Sodeau, J. R. *J. Chem. Soc., Faraday Trans.* **1992**, *88*, 1077.

(11) Kroes, G.-J.; Clary, D. C. *J. Phys. Chem.* **1992**, *96*, 7079.

(12) Robertson, S. H.; Clary, D. C. *Faraday Discuss.* **1995**, *100*, 309.

(13) Clary, D. C.; Wang, L. *J. Chem. Soc., Faraday Trans.* **1997**, *93*, 2763.

(14) Al-Halabi, A.; Kleyn, A. W.; Kroes, G.-J. *Chem. Phys. Lett.* **1999**, *307*, 505.

(15) Rieley, H.; Aslin H. D.; Haq, S. *J. Chem. Soc., Faraday Trans.* **1995**, *91*, 2349.

(16) Isakson, M. J.; Sitz, G. O. *J. Phys. Chem. A* **1999**, *103*, 2044.

(17) Andersson, P. U.; Någård, M. B.; Pettersson, J. B. C. *J. Phys. Chem. A*, in press.

(18) Haynes, D. R.; Tro, N. J.; George, S. M. *J. Phys. Chem.* **1992**, *96*, 8502.

(19) Gertner, B. J.; Hynes, J. T. *Science* **1996**, *271*, 1563.

(20) Gertner, B. J.; Hynes, J. T. *Faraday Discuss.* **1998**, *110*, 301.

(21) Bianco, R.; Gertner, B. J.; Hynes, J. T. *Bunsen-Ges. Phys. Chem.* **1998**, *102*, 518.

(22) Graham, J. D.; Roberts, J. T. *Geophys. Res. Lett.* **1995**, *22*, 251.

(23) Bolton, K.; Svanberg, M.; Pettersson, J. B. C. *J. Chem. Phys.* **1999**, *110*, 5380.

(24) Bolton, K.; Pettersson, J. B. C. *Chem. Phys. Lett.*, in press.

(25) (a) Andersson, P. U.; Någård, M. B.; Bolton, K.; Svanberg, M.; Pettersson, J. B. C., submitted to *J. Phys. Chem. A*. (b) Jenniskens, P.; Banham, S. F.; Blake, D. F.; McCoustra, M. R. S. *J. Chem. Phys.* **1997**, *107*, 1232.

(26) Field, M. J.; Bash, P. A.; Karplus, M. *J. Comput. Chem.* **1990**, *11*, 700.

(27) Eichler, U.; Kölmel, C. M.; Sauer, J. *J. Comput. Chem.* **1996**, *18*, 463.
(28) Bolton, K.; Hase, W. L.; Peslherbe, G. H. In *Multidimensional Molecular Dynamics Methods*; Thompson, D. L.; Ed.; World Scientific: New Jersey, 1998; p 143.
(29) Tuckerman, M. E.; Laasonen, K.; Sprik, M.; Parrinello, M. *J. Chem. Phys.* **1995**, *103*, 150.
(30) Laasonen, K. E.; Klein, M. L. *J. Phys. Chem. A* **1997**, *101*, 98.
(31) Buesnel, R.; Hillier, I. H.; Masters, A. J. *Chem. Phys. Lett.* **1995**, *247*, 391.
(32) Estrin, D. A.; Kohanoff, J.; Laria, D. H.; Weht, R. O. *Chem. Phys. Lett.* **1997**, *280*, 280.
(33) Jorgensen, W. L.; Chandrasekhar, J.; Madura, J. D.; Impey, R. W.; Klein, M. L. *J. Chem. Phys.* **1983**, *79*, 926.
(34) Bussolin, G.; Casassa, S.; Pisani, C.; Ugliengo, P. *J. Chem. Phys.* **1998**, *108*, 9516.
(35) Geiger, F. M.; Hicks, J. M.; deDios, A. C. *J. Phys. Chem. A* **1998**, *102*, 1514.
(36) Stewart, J. J. P. *J. Comput.-Aided Mol. Design* **1990**, *4*, 1. (MOPAC 7.0).
(37) Cummins, P. L. Molecular Orbital Program for Simulations (MOPS), 1999.
(38) Stewart, J. J. P. *J. Comput. Chem.* **1989**, *10*, 209. Stewart, J. J. P. *J. Comput. Chem.* **1989**, *10*, 221.
(39) Packer, M. J.; Clary, D. C. *J. Chem. Phys.* **1995**, *99*, 14323.
(40) Bachelo, D. E.; Binning, R. C. Jr.; Ishikawa, Y. *J. Phys. Chem. A* **1999**, *103*, 4631.
(41) Dewar, M. J. S.; Thiel, W. *J. Am. Chem. Soc.* **1977**, *99*, 4899. Dewar, M. J. S.; Thiel, W. *J. Am. Chem. Soc.* **1977**, *99*, 4907.
(42) Dewar, M. J. S.; Zoebisch, E. G.; Healy, E. F.; Stewart, J. J. P. *J. Am. Chem. Soc.* **1985**, *107*, 3902.
(43) MNDO (modified neglect of diatomic overlap) is the original MNDO-type method; AM1 and PM3 differ from MNDO primarily in the description of the core−core interactions.
(44) Jurema, M. W.; Shields, G. C. *J. Comput. Chem.* **1993**, *14*, 89.
(45) Jurema, M. W.; Kirschner, K. N.; Shields, G. C. *J. Comput. Chem.* **1993**, *14*, 1326.
(46) Plummer, P. L. M. *J. Mol. Struct.* **1997**, *417*, 35.
(47) Bash, P. A.; Ho, L. L.; MacKerell, A. D., Jr.; Levine, D.; Hallström, P. *Proc. Natl. Acad. Sci. U.S.A.* **1996**, *93*, 3698.
(48) Zerner, M. C. In *Review of Computational Chemistry*; Lipkowitz, K. B., Boyd, D. B., Eds.; VCH: 1991; Vol. 2, p 313.
(49) Rossi, I.; Truhlar, D. G. *Chem. Phys. Lett.* **1995**, *233*, 231.
(50) Bolton, K.; Hase, W. L.; Doubleday: C. Jr. *Ber. Bunsen-Ges. Phys. Chem.* **1997**, *101*, 414.
(51) Peterson, K. A.; Xantheas, S. S.; Dixon, D. A.; Dunning, T. H., Jr. *J. Phys. Chem. A* **1998**, *102*, 2449.
(52) Hodges, M. P.; Stone, A. J.; Xantheas, S. S. *J. Phys. Chem. A* **1997**, *101*, 9163.
(53) Xie, Y.; Remington, R. B.; Schaefer, H. F., III *J. Chem. Phys.* **1994**, *101*, 4878.
(54) Benedict, W. S.; Gailar, N.; Plyler, E. K. *J. Chem. Phys.* **1956**, *24*, 1139.
(55) Odutola, J. A.; Dyke, T. R. *J. Chem. Phys.* **1980**, *72*, 5062.
(56) Curtiss, L. A.; Frurip, D. J.; Blander, M. *J. Chem. Phys.* **1979**, *71*, 2703.
(57) Sears, T. J.; Bunker, P. R.; Davies, P. B.; Johnson, S. A.; Spirko, V. *J. Chem. Phys.* **1985**, *83*, 2676.
(58) Ng, C. Y.; Trevor, D. J.; Tiedemann, P. W.; Ceyer, S. T.; Kronebusch, P. L.; Mahan, B. H.; Lee, Y. T. *J. Chem. Phys.* **1977**, *67*, 4235.
(59) Dalleska, N. F.; Honma, K.; Armentrout, P. B. *J. Am. Chem. Soc.* **1993**, *115*, 12125.
(60) It should be noted that the PM3 parameters have been fitted so that the energy of a geometry-optimized molecule reproduces the experimental enthalpy of formation at 298 K. Zero point energy and thermal corrections relative to ab initio PESs can thus be regarded to be included in the parameters. Here we use the PM3 energies directly to provide a PES on which the classical trajectories are propagated.
(61) Ojamäe, L.; Shavitt, I.; Singer, S. J. *J. Chem. Phys.* **1998**, *109*, 5547.
(62) MP2 calculations show that in small (cyclic) water clusters, the O−O distances shorten considerably with increasing cluster size and reach 2.74 Å for $(H_2O)_4$, see: Xantheas, S. S.; Dunning, T. H., Jr. In *Advances in Molecular Vibrations and Collision Dynamics*; Bowman, J. M., Bacic, Z., Eds.; JAI Press: London, 1998; Vol. 3, p 281. This trend is much weaker in PM3 calculations, which yield O−O distances in $(H_2O)_4$ close to the MP2 value.
(63) Csonka, G. I.; Angyan, J. G. *J. Mol. Struct.* **1997**, *393*, 31.
(64) Planas, M.; Lee, C.; Novoa, J. J. *J. Phys. Chem.* **1996**, *100*, 16495.
(65) Re, S.; Osamura, Y.; Suzuki, Y.; Schaefer H. F., III *J. Chem. Phys.* **1998**, *109*, 973.
(66) When necessary, we will use the notation H′ for the specific hydrogen initially belonging to the HCl molecule.
(67) Kroes, G.-J. *Surf. Sci.* **1992**, *275*, 365.
(68) Batista, E. R.; Jonsson, H. In *Proceedings of the VIII Workshop of Computational Materials Science*; Ruggerone, P., Fiorentini, V., Eds.; in press.
(69) Cummins, P. E.; Gready, J. E. *Chem. Phys. Lett.* **1994**, *225*, 11.
(70) Cummins, P. E.; Gready, J. E. *J. Comput. Chem.* **1997**, *18*, 1496.
(71) Cummins, P. E.; Gready, J. E. *J. Comput. Chem.* **1998**, *19*, 977.
(72) Xantheas, S. S. *J. Chem. Phys.* **1996**, *104*, 8821.
(73) Keesee, R. G.; Castleman, A. W., Jr. *J. Phys. Chem. Ref. Data* 1986, 15, 1011.
(74) Allen, M. P.; Tildesley, D. J. *Computer Simulation of Liquids*; Clarendon Press: Oxford, 1990.
(75) Hayward, J. A.; Reimers, J. R. *J. Chem. Phys.* **1997**, *106*, 1518.
(76) Svanberg, M. *Mol. Phys.* **1997**, *92*, 1085.
(77) Xu, G.-Q.; Bernasek, S. L.; Tully, J. C. *J. Chem. Phys.* **1988**, *88*, 3376.
(78) DePristo, A. E.; Metiu, H. *J. Chem. Phys.* **1989**, *90*, 1229.
(79) Berendsen, H. J. C.; Postma, J. P. M.; vanGunsteren, W. F.; DiNola, A.; Haak, J. R. *J. Phys. Chem.* **1984**, *81*, 3684.
(80) Complications arising when starting the simulation with a metastable cluster, in which the subsequent transition to a lower-energy structure may release a considerable amount of energy, have been pointed out previously[81,82] and could substantially alter the mechanism as well as probability of HCl ionization.
(81) Wales, D. J.; Ohmine, I. *J. Chem. Phys.* **1993**, *98*, 7245.
(82) Svanberg, M.; Pettersson, J. B. C. *J. Phys. Chem. A* **1998**, *102*, 1865.
(83) Kelterbaum, R.; Kochanski, E. *J. Phys. Chem.* **1995**, *99*, 12493.
(84) Although HCl ionization within 100 ps is unlikely at 100 K (compared to 150 and 200 K), we show data from such a trajectory since the small thermal fluctuations enable important features to be illustrated more clearly.
(85) Tabazadeh, A.; Turco, R. P. *J. Geophys. Res.* **1993**, *98* D7, 12727.
(86) Graham, J. D.; Roberts, J. T. *J. Phys. Chem.* **1994**, *98*, 5974.
(87) Weast, R. C., Ed.; *Handbook of Chemistry and Physics*, 50th Edition; Chemical Rubber Co.: Cleveland, 1969.
(88) With a complete proton disorder, consistent with the Bernal−Fowler ice rules, the probability that a given hexagon on an ideal surface should be type III is less than 1/8. The same holds for type IV sites.
(89) Robinson, G. W.; Zhu, S.-B.; Singh, S.; Evans, M. W. *Water in Biology, Chemistry and Physics: Experimental Overviews and Computational Methodologies*; World Scientific: Singapore, 1996.
(90) QCISD(T)/6-311+G** energies of the optimized MP2/6-311+G** structures of $HCl(H_2O)_4$ predicts the lowest energy ionized structure to be 6 kJ/mol above the molecular structure.[40]
(91) Lobaugh, J.; Voth, G. A. *J. Chem. Phys.* **1996**, *104*, 2056.
(92) Kobayashi, C.; Iwahashi, K.; Saito, S.; Ohmine, I. *J. Chem. Phys.* **1996**, *105*, 6358.
(93) Cheng, H.-P. *J. Phys. Chem. A* **1998**, *102*, 6201.
(94) Delzeit, L.; Powell, K.; Uras, N.; Devlin, J. P. *J. Phys. Chem. B* **1997**, *101*, 2327.
(95) Uras, N.; Rahman, M.; Devlin, J. P. *J. Phys. Chem. B* **1998**, *102*, 9375.
(96) MacTaylor, R. S.; Gilligan, J. J.; Moody, D. J.; Castleman, A. W., Jr. *J. Phys. Chem. A* **1999**, *103*, 2655. MacTaylor, R. S.; Gilligan, J. J.; Moody, D. J.; Castleman, A. W., Jr. *J. Phys. Chem. A* **1999**, *103*, 4196.